

# Electromagnetic form factors of nucleons with QCD constraints: Systematic study of space- and time-like regions

Susumu Furuichi\*

*Department of Physics, Rikkyo University, Toshima, Tokyo 171-8501, Japan*

Hirohisa Ishikawa†

*Department of Economics, Meikai University, Urayasu, Chiba 279-8550, Japan*

Keiji Watanabe‡

*Department of Physics, Meisei University, Hino, Tokyo 191-8506, Japan*

(Received 6 August 2009; revised manuscript received 19 March 2010; published 30 April 2010)

Elastic electromagnetic form factors of nucleons are investigated for both the time-like and the space-like momenta by using the unsubtracted dispersion relation with QCD constraints. It is shown that the calculated form factors reproduce the experimental data reasonably well; they agree with recent experimental data for the neutron magnetic form factors for the space-like data obtained by the CLAS Collaboration and are compatible with the ratio of the electric and magnetic form factors for the time-like momentum obtained by the BABAR Collaboration.

DOI: [10.1103/PhysRevC.81.045209](https://doi.org/10.1103/PhysRevC.81.045209)

PACS number(s): 14.20.Dh, 13.40.Gp, 12.38.-t, 11.55.Fv

## I. INTRODUCTION

Recently, there have been remarkable developments in experiments for the nucleon electromagnetic form factors:

- (i) For the space-like momentum, the ratio of the electric and magnetic form factors of the proton,  $G_E^p$  and  $G_M^p$ , respectively, was shown to be a decreasing function of the squared momentum transfer,  $Q^2$ , and the experimental results imply that the proton electric form factor vanishes for  $Q^2 \approx 7$  (GeV/c)<sup>2</sup> [1–5].
- (ii) For the neutron magnetic form factor,  $G_M^n$ , very accurate experimental data were obtained and it approximately satisfies  $G_M^n(Q^2)/\mu_n \approx G_D(Q^2) = (1 + Q^2/0.71)^{-2}$ , with  $Q$  being represented in terms of GeV/c, for a fairly wide range of squared momentum transfer,  $Q^2 = 1.4$ – $4.8$  (GeV/c)<sup>2</sup> [6,7] (CLAS Collaboration).
- (iii) For the time-like momentum the ratio  $|G_E^p/G_M^p|$  was estimated [8,9], (BABAR Collaboration), whereas previously the data of form factors had been analyzed under the assumption  $G_E^p = 0$  or  $G_E^p = G_M^p$ .

Asymptotically, the experimental data of nucleon form factors decrease more rapidly than the dipole formula for large  $Q^2$  and the decrease has been understood as a realization of perturbative QCD [10]. According to perturbative QCD the nucleon form factors decrease for large momentum transfer, for both space-like and time-like momenta.

To realize QCD properties by dispersion theory, use is made of the unsubtracted dispersion relation with the superconvergence conditions [11,12]. Because of the analyticity property of the dispersion relation, the form factor for the time-like momentum transfer,  $t > 0$ , is obtained by the analytic continuation from the space-like part,  $t < 0$ , so that we are able to investigate systematically the form factors for the space- and time-like momentum transfers.

Theoretical calculations of  $G_M^n$  turned out to be larger than the aforementioned new experimental data for  $Q^2 = 1.4$ – $4.8$  (GeV/c)<sup>2</sup> (see Ref. [7]). It is important to confirm whether it is possible to realize the experimental data simply by the adjustment of parameters or by the refinement of absorptive parts.

It is the purpose of this paper to analyze experimental data of nucleon form factors by dispersion theory, with the QCD constraints imposed, by taking account of these new experimental results.

Organization of the paper is given as follows: In Sec. II we explain the superconvergent dispersion relation and give conditions that are used in this paper. In Sec. III we summarize the absorptive parts, which are broken up into three parts: low-momentum, intermediate-momentum, and asymptotic regions. For each momentum region the imaginary parts are given. The asymptotic part is expressed as an expansion in terms of the analytically regularized effective coupling constant in the renormalization group for QCD. In Sec. IV we remark on the numerical analysis. In Sec. V numerical results are summarized. The final section is devoted to a general discussion.

## II. SUPERCONVERGENT DISPERSION RELATION

As mentioned in Sec. I, the electromagnetic form factors approach zero asymptotically for  $t \rightarrow \infty$ . Therefore, we

\*Sengencho 3-2-6, Higashikurume, Tokyo 203-0012, Japan.

†ishikawa@meikai.ac.jp

‡keijiwatanabe888@yahoo.co.jp; Akazutumi, 5-36-2, Setagaya, Tokyo 156-0044, Japan.

assume the unsubtracted dispersion relations for charge and magnetic moment form factors  $F_1^I$  and  $F_2^I$ , respectively, with  $I$  denoting the isospin state  $I = 0, 1$ ; that is,

$$F_i^I = \frac{1}{\pi} \int_{t_0}^{\infty} dt' \frac{\text{Im} F_i^I(t')}{t' - t}, \quad (1)$$

where the threshold is  $t_0 = 4\mu^2$ . Here  $\mu$  is the pion mass, being taken as the average of the neutral and charged pion masses.

We impose the superconvergence conditions for  $\text{Im} F_i^I$ :

$$\frac{1}{\pi} \int_{t_0}^{\infty} dt' \text{Im} F_1^I(t') = \frac{1}{\pi} \int_{t_0}^{\infty} dt' t' \text{Im} F_1^I(t') = 0, \quad (2)$$

$$\begin{aligned} \frac{1}{\pi} \int_{t_0}^{\infty} dt' \text{Im} F_2^I(t') &= \frac{1}{\pi} \int_{t_0}^{\infty} dt' t' \text{Im} F_2^I(t') \\ &= \frac{1}{\pi} \int_{t_0}^{\infty} dt' t'^2 \text{Im} F_2^I(t') \\ &= 0, \end{aligned} \quad (3)$$

where  $\text{Im} F_i^I(t')$  satisfies the asymptotic conditions for  $t' \rightarrow \infty$ :

$$t'^i \text{Im} F_i^I(t') \rightarrow c / [\ln(t'/Q_0^2)]^{\gamma+1} \quad (i = 1, 2), \quad (4)$$

with  $Q_0$ ,  $\gamma (\geq 2)$ , and  $c$  as constants. The constant  $\gamma$  is written in terms of the anomalous dimension of the renormalization group in QCD. In this calculation we take  $\gamma = 2$  so that  $F_i^I$ , being given by Eq. (1) with the superconvergence conditions (2) and (3), satisfy the asymptotic conditions of QCD:

$$F_i(t) \rightarrow c / \{\pi \gamma t^{i+1} [\ln(|t|/Q_0^2)]^\gamma\} \quad (i = 1, 2) \quad (5)$$

for  $t \rightarrow \pm\infty$  (see Ref. [13] for the proof of formulas and formulation).

In addition to the conditions (2) and (3) we impose the normalization conditions at  $t = 0$ :

$$\frac{1}{2} = \frac{1}{\pi} \int_{t_0}^{\infty} dt' \text{Im} F_1^I(t')/t', \quad (6)$$

$$g^I = \frac{1}{\pi} \int_{t_0}^{\infty} dt' \text{Im} F_2^I(t')/t', \quad (7)$$

where  $g^I$  is the anomalous magnetic moments of nucleons with isospin  $I$ .

### III. IMAGINARY PART OF THE FORM FACTORS

Let us discuss the imaginary parts of the nucleon form factors, which are broken up into three parts: low-momentum, intermediate-momentum, and asymptotic regions.

#### A. Low-momentum region

The imaginary parts of the form factors,  $\text{Im} F_i^V$ , are given in terms of the two-pion contribution as follows:

$$\begin{aligned} \text{Im}[F_1^V(t)/e] &= \frac{m(t - 4\mu^2)}{2(4m^2 - t)} \left( \frac{t - 4\mu^2}{t} \right)^{1/2} \\ &\times \text{Re} \left\{ M^*(t) \left[ f_+^{(-)1}(t) - \frac{t}{4m^2} \frac{m}{\sqrt{2}} f_-^{(-)1}(t) \right] \right\}, \end{aligned}$$

$$\begin{aligned} \text{Im}[2mF_2^V(t)/e] &= \frac{m(t - 4\mu^2)}{2(4m^2 - t)} \left( \frac{t - 4\mu^2}{t} \right)^{1/2} \\ &\times \text{Re} \left\{ M^* \left[ \frac{m}{\sqrt{2}} f_-^{(-)1}(t) - f_+^{(-)1}(t) \right] \right\}, \end{aligned} \quad (8)$$

where  $f_{\pm}^{(-)1}(t)$  are helicity amplitudes for  $\pi\pi \leftrightarrow N\bar{N}$ ,  $M(t)$  is the pion form factor, and  $\mu$  is the pion mass. For the helicity amplitudes we use the numerical values given by Höhler and Schopper [14] and parametrize  $M(t)$  according to

$$M(t) = t_{\rho} \{ 1 + (\Gamma_{\rho}/m_{\rho})d \} [t_{\rho} - t - im_{\rho}^2 \Gamma_{\rho} (q_t/q_{\rho})^3 / \sqrt{t}]^{-1}, \quad (9)$$

where  $m_{\rho}$  and  $\Gamma_{\rho}$  are the  $\rho$  meson mass and width, respectively, and

$$t_{\rho} = m_{\rho}, \quad q_{\rho} = \sqrt{t_{\rho} - \mu^2}, \quad q_t = \sqrt{t - \mu^2}, \quad (10)$$

$$d = \frac{3\mu^2}{\pi t_{\rho}} \ln \frac{m_{\rho} + 2q_{\rho}}{2\mu} + \frac{m_{\rho}}{2\pi q_{\rho}} \left( 1 - \frac{2\mu^2}{t_{\rho}} \right). \quad (11)$$

The imaginary parts thus obtained are denoted as  $\text{Im} F_i^H$  ( $i = 1, 2$ ) hereafter. It must be remarked that the  $\rho$  meson contribution is included in the helicity amplitudes of Ref. [14]. The uncorrelated kaon pair is neglected here as the effect was estimated to be small [15].

#### B. Intermediate-momentum region

The intermediate states  $4\mu^2 \leq t \leq \Lambda_1^2$  are approximated by the addition of the Breit-Wigner terms, with the imaginary part parametrized as follows:

$$\text{Im} f_R^{\text{BW}}(t) = \frac{g}{(t - M_R^2)^2 + g^2}, \quad (12)$$

where

$$g = \frac{\Gamma M_R^2 (M_R^2 + t_{\text{res}})^3}{(M_R^2 - t_0)^{3/2}} \sqrt{\frac{(t - t_0)^3}{t} \frac{1}{(t + t_{\text{res}})^3}}. \quad (13)$$

Here  $M_R$  and  $\Gamma$  are the mass and width of the resonance, respectively, the threshold  $t_0$  is  $t_0 = 4\mu^2$ , and  $t_{\text{res}}$  is treated as an adjustable parameter.  $g$  is introduced to cut off the Breit-Wigner formula.

We write the intermediate part as the summation of resonances,

$$\text{Im} F_i^{\text{BW},I} = \sum_n a_n^{I,i} f_{nR}^I, \quad (14)$$

where  $I$  is the isospin and  $n$  is the labeling of resonances (see Table I). Here the suffix  $i$  denotes  $i = 1, 2$ , corresponding to the charge and Pauli form factors  $F_1^N$  and  $F_2^N$  ( $N = n$  or  $p$ ). The same formulas for  $f_{nR}^I$  are used for  $i = 1$  and  $i = 2$ .

#### C. Asymptotic region

We express the form factors as a power series in the effective coupling constant of QCD,  $\alpha_S$ . To calculate the absorptive part, it is necessary to perform analytic continuation to the time-like

TABLE I. Masses and widths determined by the analysis for cases I and II.

$I$	$n$	Case I		Case II	
		mass (GeV/ $c^2$ )	width (GeV)	mass (GeV/ $c^2$ )	width (GeV)
$I = 1$	1	1.351	0.3240	1.340	0.3221
	2	1.370	0.2200	1.381	0.2199
	3	1.587	0.2640	1.618	0.2636
	4	1.827	0.3680	1.823	0.3679
	5	2.082	0.3960	2.048	0.3848
$I = 0$	1	0.78256	$0.844 \times 10^{-2}$	0.78256	$0.844 \times 10^{-2}$
	2	1.01945	$0.426 \times 10^{-2}$	1.01945	$0.426 \times 10^{-2}$
	3	1.204	0.1583	1.207	0.1584
	4	1.440	0.2075	1.438	0.2078
	5	1.509	0.1285	1.504	0.1279

momentum. Here we give only the necessary procedure for the analytic continuation of the effective coupling constant to the time-like momentum by using the analytic regularization [16–18], as the formulation is given in Ref. [13].

Let  $\alpha_S(Q^2)$  be the effective coupling constant in the renormalization group calculated by perturbative QCD as a function of the squared momentum  $Q^2$  for the space-like momentum. We use the three-loop approximation for  $\alpha_S(Q^2)$ , which is expressed in the Padé form

$$\alpha_S(Q^2) = \frac{4\pi}{\beta_0} \left\{ \ln(Q^2/\Lambda^2) + a_1 \ln[\ln(Q^2/\Lambda^2)] + a_2 \frac{\ln[\ln(Q^2/\Lambda^2)]}{\ln(Q^2/\Lambda^2)} + \frac{a_3}{\ln(Q^2/\Lambda^2)} + \dots \right\}^{-1}. \quad (15)$$

Here  $\Lambda$  is the QCD scale parameter, and  $a_i$  are expressed in terms of the  $\beta$  function of QCD,

$$a_1 = 2\beta_1/\beta_0^2, \quad a_2 = 4\frac{\beta_1^2}{\beta_0^4}, \quad a_3 = \frac{4\beta_1^2}{\beta_0^4} \left( 1 - \frac{\beta_0\beta_2}{8\beta_1^2} \right), \quad (16)$$

where

$$\beta_0 = 11 - \frac{2n_f}{3}, \quad \beta_1 = 51 - \frac{19n_f}{3}, \quad (17)$$

$$\beta_2 = 2357 - \frac{5033}{9}n_f + \frac{325}{27}n_f^2,$$

with  $n_f$  being the flavor number. We perform the analytic continuation of the squared momentum to the time-like region,  $s$ , by the replacement in (15)

$$Q^2 \rightarrow e^{-i\pi} s. \quad (18)$$

Then  $\alpha_S(e^{-i\pi} s)$  becomes complex and is expressed as follows:

$$\frac{\beta_0}{4\pi} \alpha_S(e^{-i\pi} s) = 1/(u - iv) = \frac{u + iv}{D}, \quad (19)$$

$$D = u^2 + v^2, \quad (20)$$

where  $u$  and  $v$  are given as

$$u = \ln(s/\Lambda^2) + \frac{a_1}{2} \ln[\ln^2(s/\Lambda^2) + \pi^2] + \frac{a_2}{\ln^2(s/\Lambda^2) + \pi^2} \left\{ \frac{1}{2} \ln(s/\Lambda^2) \ln[\ln^2(s/\Lambda^2) + \pi^2] + \pi\theta \right\} + \frac{a_3 \ln(s/\Lambda^2)}{\ln^2(s/\Lambda^2) + \pi^2}, \quad (21)$$

$$v = \pi + a_1\theta - \frac{a_2}{\ln^2(s/\Lambda^2) + \pi^2} \left\{ \frac{\pi}{2} \ln[\ln^2(s/\Lambda^2) + \pi^2] - \theta \ln(s/\Lambda^2) \right\} - \frac{\pi a_3}{\ln^2(s/\Lambda^2) + \pi^2}, \quad (22)$$

with

$$\theta = \tan^{-1}\{\pi/\ln(s/\Lambda^2)\}. \quad (23)$$

The effective coupling constant is given by the dispersion integral for both the space-like and the time-like momentum:

$$\alpha_R(t) = \int_0^\infty dt' \frac{\sigma(t')}{t' - t} \quad (24)$$

with

$$\sigma(t') = \text{Im} \alpha_S(e^{-i\pi} s) = 4\pi v/\beta_0 D. \quad (25)$$

The constant  $\alpha_R(t)$  represented by Eq. (24) is called the analytically regularized effective coupling constant as it has no singular point for  $t = -Q^2 < 0$ . The regularization eliminates the ghost pole of  $\alpha_S(Q^2)$ , given by Eq. (15), appearing at

$$Q^2 = Q^{*2} = \Lambda e^{u^*}, \quad (26)$$

where  $u^* = 0.7659596\dots$  for flavor number  $n_f = 3$ . Calculating the integral in Eq. (24), we find that  $\alpha_R(t)$  is approximately given by the simple formula with the ghost pole subtracted,

$$\alpha_R(Q^2) \approx \alpha_S(Q^2) - A^*/(Q^2 - Q^{*2}), \quad (27)$$

where the residue  $A^*$  is

$$A^* = 4\pi \Lambda^2 e^{u^*} / \left[ \beta_0 \left( 1 + \frac{a_1}{u^*} - a_2 \frac{\ln u^*}{u^{*2}} + \frac{a_2 - a_1}{u^{*2}} \right) \right]. \quad (28)$$

We use Eq. (27) as the regularized coupling constant; for the time-like momentum we replace  $Q^2 \rightarrow e^{-i\pi} s$  in Eq. (27) as was mentioned before.

The QCD parts,  $F_i^{\text{QCD}, I}$  ( $i = 1, 2; I = 0, 1$ ) for the squared time-like momentum are written as follows:

$$F_i^{\text{QCD}, I}(s) = \hat{F}_i^{\text{QCD}, I}(s) h_i(s), \quad (29)$$

where  $\hat{F}_i^{\text{QCD}, I}$  are given as an expansion in terms of the effective coupling constant,

$$\hat{F}_i^{\text{QCD}, I}(s) = \sum_{j \geq 2} c_j^{\text{QCD}, I} \{\alpha_R(s)\}^j, \quad (30)$$

for the time-like squared momentum  $s$ . We multiply by the function  $h(s)$  in Eq. (29) to ensure the convergence of

the superconvergence conditions (2) and (3). The following formula is assumed for  $h_i(s)$ :

$$h_i(s) = \left( \frac{s - t_Q}{s + t_1} \right)^{3/2} \left( \frac{t_2}{s + t_2} \right)^{i+1}, \quad (31)$$

which may be interpreted as the form factor for  $\gamma \rightarrow q\bar{q}$  with  $t_Q$  being the threshold of the quark antiquark pair. The parameters  $t_Q$ ,  $t_1$ , and  $t_2$  are taken as adjustable parameters and will be determined by the analysis of experimental data.

For the time-like momentum, we perform the analytic continuation of the regularized effective coupling constant  $\alpha_R(Q^2)$  to  $\alpha_R(s)$  through the equation

$$\alpha_R(s) = \alpha_R(Q^2 e^{-i\pi}) = \text{Re}[\alpha_R(s)] + i \text{Im}[\alpha_R(s)]. \quad (32)$$

The summation in Eq. (30) begins in the second order in the effective coupling constant so as to realize the logarithmic decrease of the nucleon form factors [Eq. (5)]. It is remarked here that  $\text{Re} \alpha_R(s) \rightarrow \text{const}/[\ln(s/\Lambda^2)]$  and  $\text{Im} \alpha_R(s) \rightarrow \text{const}/[\ln(s/\Lambda^2)]^2$  for  $s \rightarrow \infty$  so that  $\text{Im} F$  satisfies condition (4).

The imaginary part of Eq. (30) is obtained as

$$\begin{aligned} \text{Im} \hat{F}_i^{\text{QCD}, I} &= 2c_{i,2}^{\text{QCD}, I} \text{Re} \alpha_R \text{Im} \alpha_R \\ &+ c_{i,3}^{\text{QCD}, I} [3(\text{Re} \alpha_R)^2 \text{Im} \alpha_R - (\text{Im} \alpha_R)^3] \\ &+ c_{i,4}^{\text{QCD}, I} [4(\text{Re} \alpha_R)^3 \text{Im} \alpha_R - 4\text{Re} \alpha_R (\text{Im} \alpha_R)^3] \\ &+ \dots, \end{aligned} \quad (33)$$

and

$$\text{Im} F_i^{\text{QCD}, I}(s) = \text{Im} \hat{F}_i^{\text{QCD}, I}(s) h_i(s). \quad (34)$$

We write the low-energy part, intermediate resonance part, and asymptotic QCD parts of form factors as  $F_i^{\text{H}}$ ,  $F_i^{\text{BW}, I}$ , and  $F_i^{\text{QCD}, I}$ , respectively, which are given by the dispersion integral with the imaginary parts from Eqs. (8), (14) and (34):  $F_i^{\text{H}}$  denote the parts obtained by using the helicity amplitudes of Höhler and Schopper. The form factors  $F_i^I$  are defined by adding them up. We impose the conditions or Eqs. (2) and (3) on  $\text{Im} F_i^I$  so that the QCD conditions are satisfied.

#### IV. NUMERICAL ANALYSIS

We analyzed the experimental data of nucleon electromagnetic form factors for the space-like momentum,  $G_M^p/\mu_p G_D$ ,  $G_E^p/G_D$ ,  $G_M^n/\mu_n G_D$ , and  $G_E^n$ , and the ratio  $\mu_p G_E^p/G_M^p$  and for the time-like momentum,  $|G^p|$  and  $|G^n|$ , in Refs. [19]–[41] and the aforementioned recent experimental data,  $G_M^n$ , for the space-like momentum and  $|G_E^p/\mu_p G_M^p|$  for the time-like momentum. The parameters appearing in the formulas are determined so as to minimize  $\chi^2$ .

As was mentioned in Sec. I we analyze by taking account of the recent experimental data: (a)  $|\mu_p G_E^p/G_M^p|$  for the time-like momentum (BABAR Collaboration) and (b)  $G_M^n$  for  $Q^2 = 1\text{--}4.8$  (GeV/c)<sup>2</sup> (CLAS Collaboration).

To see how the situation changes by taking account of these new experiments in addition to the other data, we perform analysis for the following two cases in the chi-square analysis:

Case I: Only the data (a)  $|\mu_p G_E^p/G_M^p|$  for the time-like momentum are added.

Case II: Both of the experimental data, (a)  $|\mu_p G_E^p/G_M^p|$  for the time-like momentum and (b) new data for  $G_M^n$  for the space-like momentum, are added.

Let us remark on the experiments for the time-like momentum [8,32,34], where the form factors  $|G^p|$  and  $|G^n|$  are determined by using the formula for the cross section  $\sigma_0$  for the processes  $e + \bar{e} \rightarrow N + \bar{N}$  or  $N + \bar{N} \rightarrow e + \bar{e}$ , which is given as

$$\sigma_0 = \frac{4\pi\alpha^2\nu}{3s} \left( 1 + \frac{2m_p^2}{s} \right) |G(s)|^2. \quad (35)$$

Here  $\alpha$  is the fine-structure constant and  $\nu$  is the nucleon velocity. The form factors  $|G_M^N|$  are estimated from  $|G|$  under the assumption  $G_M = G_E$  or  $G_E = 0$ . The cross section  $\sigma_0$  is expressed in terms of  $G_M^N$  and  $G_E^N$  as follows:

$$\sigma_0 = \frac{4\pi\alpha^2\nu}{3s} \left( |G_M^N|^2 + \frac{2m^2}{s} |G_E^N|^2 \right). \quad (36)$$

Equating (35) and (36), we have

$$|G|^2 = \frac{|G_M^N|^2 + 2m^2 |G_E^N|^2/s}{1 + 2m^2/s}. \quad (37)$$

TABLE II. The coefficients  $a_i^{I,n}$ , residues at the resonance poles, determined by the  $\chi^2$  analysis for cases I and II.

$I$	$n$	Case I		Case II	
		$a_1^{I,n}$ (GeV <sup>2</sup> )	$a_2^{I,n}$ (GeV <sup>2</sup> )	$a_1^{I,n}$ (GeV <sup>2</sup> )	$a_2^{I,n}$ (GeV <sup>2</sup> )
$I = 1$	1	-4.49	8.07	-4.54	8.01
	2	7.38958	-15.38252	7.95421	-16.42955
	3	-7.782044	10.39096	-9.342846	10.93951
	4	6.078791	-5.890514	7.199141	-7.383261
	5	-1.34	1.28	-1.41	1.42
$I = 0$	1	0.9018172	0.05832291	0.9125511	0.02062334
	2	-3.999109	0.8816084	-3.898647	0.6904565
	3	8.122170	-2.890431	7.988233	-2.256377
	4	-4.549486	-1.191009	-5.013229	-0.7494913
	5	-0.8224076	3.347816	-0.3145762	2.44927

Substituting our calculated result of form factors into the right-hand side of Eq. (37), we obtain the theoretical value for  $|G|$ , which is compared with the experimental data for the magnetic form factor obtained under the assumption  $G_M = G_E$ .

The parameters appearing in our analysis are the following: residues at resonances, coefficients appearing in the expansion by the QCD effective coupling constants, and cutoffs for the intermediate region  $\Lambda_1$ . In addition to them we have parameters in the Breit-Wigner formula and the convergence factor  $h$  of the QCD contribution,  $t_0$ ,  $t_{\text{res}}$ ,  $t_1$ ,  $t_2$ , and  $t_3$ .

We have taken the masses and the widths of resonances as adjustable parameters. As the superconvergence constraints impose very stringent conditions on the form factors, it is necessary to take the masses and widths as parameters.

## V. NUMERICAL RESULTS

We give in Tables I, II, and III the results for the parameters for cases I and II obtained by the chi-square analysis; Table I lists the masses and widths of resonances, Table II lists residues at resonance poles, and Table III lists the coefficients  $c_{i,j}^{\text{QCD},I}$  ( $i = 1, 2$ ;  $j = 2, 3, 4$ ;  $I = 0, 1$ ) in the expansion in terms of the effective coupling constant  $\alpha_R$  of QCD defined by Eq. (24). The flavor number is taken as  $n_f = 3$ .  $\text{Im}F_i^H$  is cut off at  $\Lambda_0^2 = 0.779 \text{ GeV}^2$  and the Breit-Wigner formulas at  $\Lambda_1 = 26.0 \text{ GeV}$ . The QCD parameter is fixed at  $\Lambda = 0.216 \text{ GeV}$ . The other parameters are determined as follows:

Case I:  $t_0 = 4\mu^2$ ,  $t_1 = 0.243 \times 10^3 \text{ GeV}^2$ ,  $t_2 = 0.237 \times 10^3 \text{ GeV}^2$ ,  $t_{\text{res}} = 0.2260 \times 10^3 \text{ GeV}^2$ , and  $t_Q = 0.202 \times 10^2 \text{ GeV}^2$ .

Case II: The same as in case I except for  $t_{\text{res}} = 0.2300 \times 10^3 \text{ GeV}^2$ .

The value of  $\chi^2$  is obtained as  $\chi_{\text{tot}}^2 = 446.6$  for case I and  $\chi_{\text{tot}}^2 = 524.5$  for case II, which includes the data of both space-like and time-like regions. The total numbers of data points are 243 for case I and 252 for case II. The number of parameters is 36 so that  $\chi_{\text{min}}/(\text{degree of freedom}) = 2.0$  for case I and 2.5 for case II.

TABLE III. The coefficients  $c_{i,j}^{\text{QCD},I}$  of the QCD terms for cases I and II determined by the  $\chi^2$  analysis.

$I$	$i$	Case I		
		$c_{i,2}^{\text{QCD},I}$	$c_{i,3}^{\text{QCD},I}$	$c_{i,4}^{\text{QCD},I}$
$I = 1$	1	-1.142469	$0.1105 \times 10^2$	-7.100
	2	4.316448	$-0.4454 \times 10^2$	$0.5657 \times 10^2$
$I = 0$	1	1.176993	-2.36	$-0.8114 \times 10^2$
	2	-6.4872	$0.7802 \times 10^2$	$-0.19375 \times 10^3$
$I$	$i$	Case II		
		$c_{i,2}^{\text{QCD},I}$	$c_{i,3}^{\text{QCD},I}$	$c_{i,4}^{\text{QCD},I}$
$I = 1$	1	0.5942862	-4.431	-7.35
	2	3.337350	$-0.3614 \times 10^2$	$0.6112 \times 10^2$
$I = 0$	1	0.4515128	2.81	$-0.6793 \times 10^2$
	2	-5.50069	$0.69220 \times 10^2$	$-0.195220 \times 10^3$

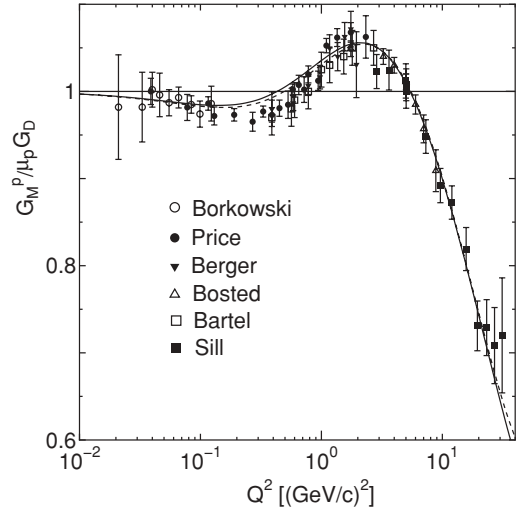


FIG. 1. Proton magnetic form factor for the space-like momentum. The solid curve is the result for case I and the dashed one for case II. The data are taken from Borkowski *et al.* [35], Price *et al.* [38], Berger *et al.* [37], Bosted *et al.* [19], Bartel *et al.* [39], and Sill *et al.* [40].

We illustrate in Figs. 1–10 the calculated results for the form factors. The results for case I are given by the solid curves and those for case II by the dashed ones. In Figs. 1–5 the results for the space-like momentum are illustrated. Figure 1 shows the proton magnetic form factors  $G_M^p/\mu_p G_D$ , Fig. 2 shows proton electric form factor  $G_E^p/G_D$ , Fig. 3 shows the neutron magnetic form factor  $G_M^n/\mu_n G_D$ , and Fig. 4 shows the neutron electric form factor. In Fig. 5 we illustrate the ratio of proton electric and proton magnetic form factors,  $\mu_p G_E^p/G_M^p$ . We find that  $G_E^p = 0$  at  $Q^2 = 6.60 \text{ (GeV/c)}^2$  for case I and  $Q^2 = 6.12 \text{ (GeV/c)}^2$  for case II. The form factor for the time-like momentum,  $|G|$ , is given for the proton in Fig. 6 ( $s \leq 15 \text{ GeV}^2$ ) and Fig. 7 ( $s < 5 \text{ GeV}^2$ ). In Fig. 8  $|G|$

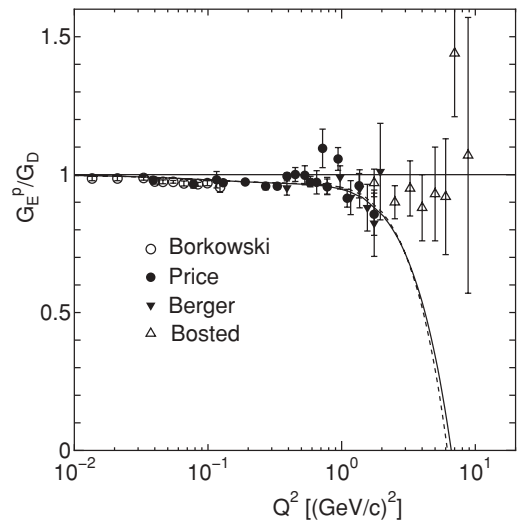


FIG. 2. Proton electric form factor for the space-like momentum. The solid curve is the result for case I and the dashed one for case II. The data points are taken from Berger *et al.* [37], Price *et al.* [38], Borkowski *et al.* [35], and Bosted *et al.* [19].

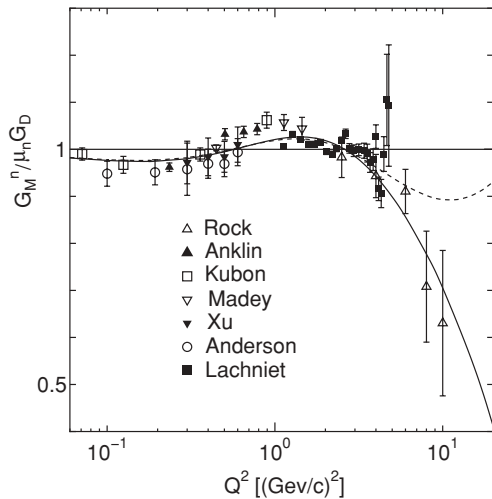


FIG. 3. Neutron magnetic form factors for the space-like momentum. The solid curve is the result for case I and the dashed one for case II. The data points are taken from Rock *et al.* [20], Anklin *et al.* [21], Kubon *et al.* [28], Madey *et al.* [41], Xu *et al.* [29], Anderson *et al.* [6], and Lachniet *et al.* [7].

is illustrated for the neutron. The result for the proton form factor agrees with the experimental data, but for the neutron the calculated one becomes larger than the experimental values for large  $Q^2$ . In Fig. 9 we compare the calculated result for the neutron magnetic form factor  $G_M^n / \mu_n G_D$  with the recent experiments [6,7]. The dashed curve (case II) agrees with the experimental data very well. The solid one (case I) becomes a little larger than the data of the CLAS Collaboration. However, the deviation is not too large. In Fig. 10 we illustrate the result for  $|G_E^p / \mu_p G_M^p|$  for the time-like momentum. There seems to be some discrepancy between the experimental data: The ratio obtained by Bardin *et al.* [8] is smaller than that of Aubert

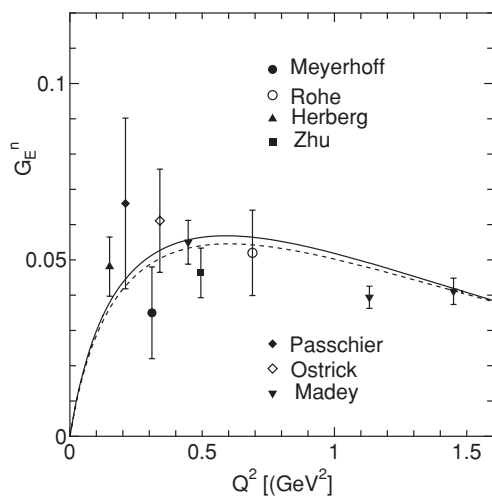


FIG. 4. Neutron electric form factor for the space-like momentum. The solid curve is the result for case I and the dashed one for case II. Data points are taken from Meyerhoff *et al.* [22], Rohe *et al.* [30], Herberg *et al.* [24], Zhu *et al.* [31], Passchier *et al.* [25], Ostrick *et al.* [26], and Madey *et al.* [41].

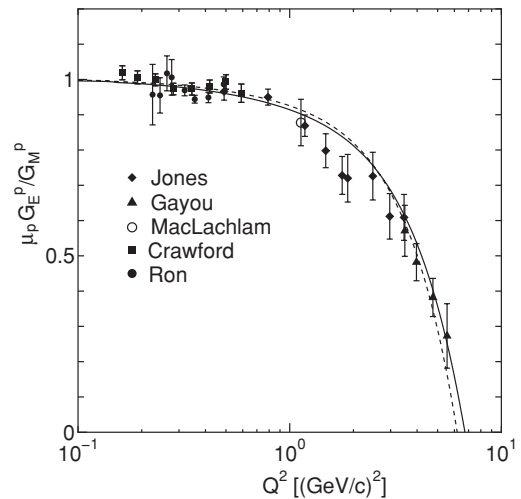


FIG. 5. Ratio of the electric and magnetic form factors of proton for the space-like momentum. The solid curve is the result for case I and the dashed one for case II. Data points are taken from Jones *et al.* [1], Gayou *et al.* [2], MacLachlam *et al.* [3], Crawford *et al.* [4], and Ron *et al.* [5].

*et al.* [9]. Our result coincides with the result of Bardin *et al.* for small  $Q^2$  and that of Aubert *et al.* for large  $Q^2$ .

## VI. CONCLUDING REMARKS

We have shown that the experimental data of the nucleon form factors are reproduced reasonably well by the dispersion relation with superconvergence conditions both for the space-like and time-like momentum transfer. In our calculations we take on a model for the imaginary part of the form factors,  $\text{Im}F$ , being given as an addition of the low, intermediate, and asymptotic parts of QCD. All of the parameters are contained

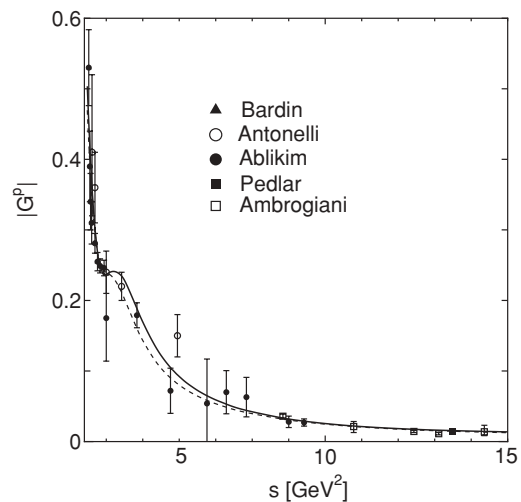


FIG. 6. Proton form factors for the time-like momentum. The solid curve is the result for case I and the dashed one for case II. The data points are taken from Bardin *et al.* [8], Antonelli *et al.* [34], Ablikim *et al.* [32], and Pedlar *et al.* [33]. The data of Aubert *et al.* [9] are given in Fig. 7.

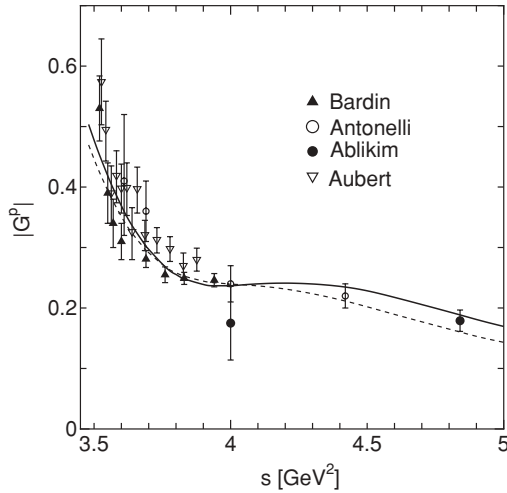


FIG. 7. Proton form factors for the time-like momentum for  $s < 5 \text{ GeV}^2$ . The solid curve is the result for case I and the dashed one for case II. The curves and data points are the same as in Fig. 6 with the addition of Aubert *et al.* [9].

in  $\text{Im}F$ . In the calculations performed by Belushkin *et al.* [12], they gave models for the form factor  $F$  itself, which satisfy the unsubtracted dispersion relation with the superconvergence condition. The parameters are contained in  $F$ .

In our formulation  $\text{Im}F^{\text{QCD}}$  is separated from the other parts, so that we are able to determine the QCD contribution to the form factors.  $\text{Im}F^{\text{QCD}}$  is assumed to be given as an expansion by the effective coupling constant of the renormalization group of QCD and the coefficients are determined by a chi-square analysis. It is concluded that an approximation up to third order in the effective coupling constant is required as in the case of deep inelastic lepton hadron interactions; that is, the next to the leading order is necessary. The same conclusion had been reached for the pion and the kaon form factors [13].

We have performed two kind of analysis, cases I and II; in the former the  $G_M^n$  data obtained by the CLAS Collaboration

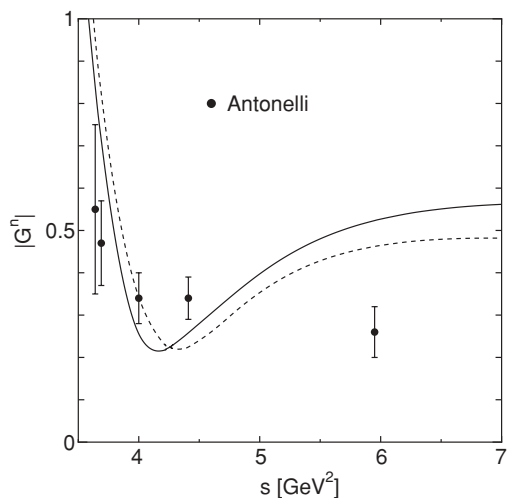


FIG. 8. The neutron form factor for the time-like momentum. The solid curve is the result for case I and the dashed one for case II. Data are taken from Antonelli *et al.* [34].

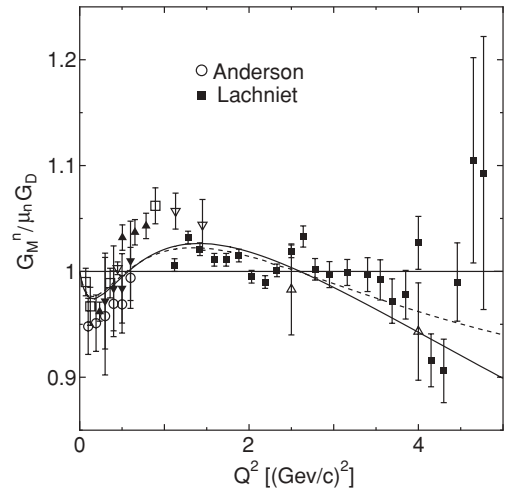


FIG. 9. Neutron magnetic form factor for the space-like momentum in the few  $(\text{GeV}/c)^2$  region. The solid curve is the result for case I and the dashed one for case II. Data are taken from Anderson *et al.* [6] and Lachniet *et al.* [7]. The same notations are used as in Fig. 3.

[7] are left out and in the latter the CLAS data are used in the chi-square analysis. Although the CLAS data, for  $Q^2 < 5 (\text{GeV}/c)^2$ , are reproduced very well by case II, there arises some disagreement for  $G_M^n$  with the data obtained by Rock *et al.* [20] at  $Q^2 = 8$  and  $10 (\text{GeV}/c)^2$ ; the calculated result for case II became larger (see Fig. 3) than the experimental value. Considering the value of  $\chi^2$ , we may conclude that case I is better than case II.

For the electric form factor of the proton there are deviations of the dispersion theoretical calculation from the experimental data for large  $Q^2$ , where the data were obtained by using the Rosenbluth formula. The discrepancy may imply the necessity of correction of two-photon processes to the experimental data [42,43].

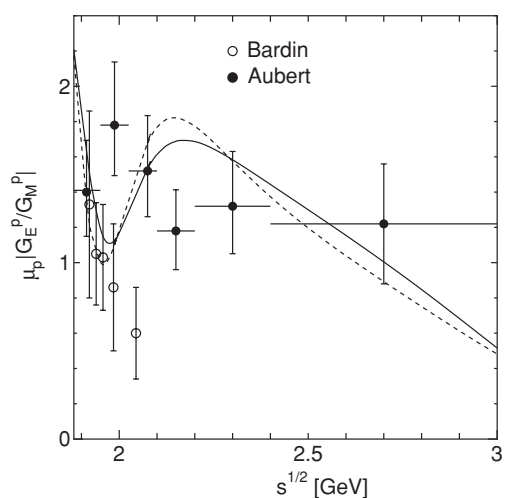


FIG. 10.  $|G_E^p / \mu_p G_M^p|$  for the time-like momentum. The solid curve is the result for case I and the dashed one for case II. The data points are taken from Bardin *et al.* [8] and Aubert *et al.* [9].

In our calculation we treated all of the vector boson masses and widths as parameters. If they are kept at experimental values, we get poor results. The superconvergence conditions are so strong that the value of  $\chi^2$  is very sensitive to the masses and widths. The masses are obtained to be smaller than the experimental value and the existence of vector bosons with masses around 1.2–1.4 GeV/ $c^2$  are necessary for both the  $I = 1$  and  $I = 0$  states.

To conclude the paper we remark on vector bosons with mass around 1.2 GeV/ $c^2$ . We have introduced the vector boson to supplement the lack of information on the unphysical

region with small  $s$ . However, for both  $I = 0$  and  $I = 1$  states there are indications of resonances observed by the processes  $e^+e^- \rightarrow \eta\pi^+\pi^-$ ,  $\gamma p \rightarrow \omega\pi^0 p$ , and  $B \rightarrow D^*\omega\pi^-$  [44].

## ACKNOWLEDGMENTS

The authors wish to express gratitude to Professor M. Ishida for valuable discussions and comments. We also would like to thank Dr. T. Komada for information on the vector bosons with mass around 1.2 GeV/ $c^2$ .

- 
- [1] M. K. Jones *et al.*, *Phys. Rev. Lett.* **84**, 1398 (2000).  
 [2] O. Gayou *et al.*, *Phys. Rev. Lett.* **88**, 092301 (2002).  
 [3] G. MacLachlan *et al.*, *Nucl. Phys. A* **764**, 261 (2006).  
 [4] C. B. Crawford *et al.*, *Phys. Rev. Lett.* **98**, 052301 (2007).  
 [5] G. Ron *et al.*, *Phys. Rev. Lett.* **99**, 202002 (2007).  
 [6] B. Anderson *et al.*, *Phys. Rev. C* **75**, 034003 (2007).  
 [7] J. Lachniet *et al.*, *Phys. Rev. Lett.* **102**, 192001 (2009).  
 [8] G. Bardin *et al.*, *Nucl. Phys. B* **411**, 3 (1994).  
 [9] B. Aubert *et al.*, *Phys. Rev. D* **73**, 012005 (2006); **73**, 071103 (2006).  
 [10] S. J. Brodsky and G. R. Farrar, *Phys. Rev. Lett.* **31**, 1153 (1973); *Phys. Rev. D* **11**, 1309 (1975); G. P. Lepage and S. J. Brodsky, *ibid.* **22**, 2157 (1980); V. L. Chernyak and I. R. Zhitnitsky *Nucl. Phys. B* **246**, 52 (1984).  
 [11] S. Furuichi and K. Watanabe, *Prog. Theor. Phys.* **82**, 581 (1989); P. Mergell, U.-G. Meißner, and D. Drechsel, *Nucl. Phys. A* **596**, 367 (1996).  
 [12] M. A. Belushkin, H.-W. Hammer, and U.-G. Meissner, *Phys. Rev. C* **75**, 035202 (2007).  
 [13] M. Nakagawa and K. Watababe, *Nouvo Cimento A* **112**, 873 (1999); *Phys. Rev. C* **61**, 055207 (2000); M. Nakagawa, H. Ishikawa, and K. Watanabe, *Acta Phys. Pol. B* **31**, 2539 (2000). K. Watanabe, H. Ishikawa, and M. Nakagawa, [arXiv:hep-ph/0111168](https://arxiv.org/abs/hep-ph/0111168).  
 [14] G. Höhler and H. H. Schopper, Landolt Börnstein, New Series Group I, Vol. 9b, p. 405. Pion Nucleon Scattering Part 2. *Methods and Results of Phenomenological Analyses*, edited by K.-H. Hellwege (Springer-Verlag, Berlin, Heidelberg, New York, 1983).  
 [15] S. Furuichi and K. Watanabe, *Prog. Theor. Phys.* **92**, 339 (1994).  
 [16] H. F. Jones and I. L. Solovstov, *Phys. Lett. B* **349**, 519 (1995).  
 [17] Yu. L. Dokshitzer and B. R. Webber, *Phys. Lett. B* **352**, 451 (1995).  
 [18] Yu. L. Dokshitzer, G. Marchesini, and B. R. Webber, *Nucl. Phys. B* **469**, 93 (1996).  
 [19] P. E. Bosted *et al.*, *Phys. Rev. C* **42**, 38 (1990).  
 [20] S. Rock *et al.*, *Phys. Rev. Lett.* **49**, 1139 (1982).  
 [21] H. Anklin *et al.*, *Phys. Lett. B* **428**, 248 (1998).  
 [22] M. Meyerhoff *et al.*, *Phys. Lett. B* **327**, 201 (1994).  
 [23] J. Becker *et al.*, *Eur. Phys. J. A* **6**, 329 (1999).  
 [24] C. Herberg *et al.*, *Eur. Phys. J. A* **5**, 131 (1999).  
 [25] I. Passchier *et al.*, *Phys. Rev. Lett.* **82**, 4988 (1999).  
 [26] M. Ostrick *et al.*, *Phys. Rev. Lett.* **83**, 276 (1999).  
 [27] C. Herberg *et al.*, *Eur. Phys. J. A* **5**, 131 (1999).  
 [28] G. Kubon *et al.*, *Phys. Lett. B* **524**, 26 (2002).  
 [29] W. Xu *et al.*, *Phys. Rev. C* **67**, 012201(R) (2003).  
 [30] D. Rohe *et al.*, *Phys. Rev. Lett.* **83**, 4257 (1999).  
 [31] H. Zhu *et al.*, *Phys. Rev. Lett.* **87**, 081801 (2001).  
 [32] M. Ablikim *et al.*, *Phys. Lett. B* **630**, 14 (2005).  
 [33] T. K. Pedlar *et al.*, *Phys. Rev. Lett.* **95**, 261803 (2005).  
 [34] A. Antonelli *et al.*, *Nucl. Phys. B* **517**, 3 (1998).  
 [35] F. Borkowski *et al.*, *Nucl. Phys. B* **93**, 461 (1975).  
 [36] P. E. Bosted *et al.*, *Phys. Rev. Lett.* **68**, 3841 (1992).  
 [37] Ch. Berger *et al.*, *Phys. Lett. B* **35**, 87 (1971).  
 [38] L. E. Price *et al.*, *Phys. Rev. D* **4**, 45 (1971).  
 [39] W. Bartel *et al.*, *Nucl. Phys. B* **58**, 429 (1973).  
 [40] A. F. Sill *et al.*, *Phys. Rev. D* **48**, 29 (1993).  
 [41] R. Madey *et al.*, *Phys. Rev. Lett.* **91**, 122002 (2003).  
 [42] D. Borisyuk and A. Kobushkin, *Phys. Rev. C* **76**, 022201(R) (2007).  
 [43] M. A. Belushkin, H.-W. Hammer, and U.-G. Meissner, *Phys. Lett. B* **658**, 138 (2008).  
 [44] On the vector boson with the mass around 1.3 GeV<sup>2</sup>, see T. Komada, [hep-ph/0612339](https://arxiv.org/abs/hep-ph/0612339); W.-M. Yao *et al.* (Particle Data Group), *J. Phys. G* **33**, 1 (2006).